The Contribution of Different Cortical Regions to the Control of Spatially Decoupled Eye–Hand Coordination

Patricia F. Sayegh[1], Diana J. Gorbet[1,2], Kara M. Hawkins[3], Kari L. Hoffman[1,2], and Lauren E. Sergio[1,2]

Abstract

■ Our brain's ability to flexibly control the communication between the eyes and the hand allows for our successful interaction with the objects located within our environment. This flexibility has been observed in the pattern of neural responses within key regions of the frontoparietal reach network. More specifically, our group has shown how single-unit and oscillatory activity within the dorsal premotor cortex (PMd) and the superior parietal lobule (SPL) change contingent on the level of visuomotor compatibility between the eyes and hand. Reaches that involve a coupling between the eyes and hand toward a common spatial target display a pattern of neural responses that differ from reaches that require eye–hand decoupling. Although previous work examined the altered spiking and oscillatory activity that occurs during different types of eye–hand compatibilities, they did not address how each of these measures of neurological activity interacts with one another. Thus, in an effort to fully characterize the relationship between oscillatory and single-unit activity during different types of eye–hand coordination, we measured the spike–field coherence (SFC) within regions of macaque SPL and PMd. We observed stronger SFC within PMdr and superficial regions of SPL (areas 5/PEc) during decoupled reaches, whereas PMdc and regions within SPL surrounding medial intrapareital sulcus had stronger SFC during coupled reaches. These results were supported by meta-analysis on human fMRI data. Our results support the proposal of altered cortical control during complex eye–hand coordination and highlight the necessity to account for the different eye–hand compatibilities in motor control research. ■

INTRODUCTION

The brain's ability to perform various types of visually guided reaches enables our interactions with the objects around us. This behavior is so critical that basic reaching movements, in which the eyes and the hand move toward a common goal, are not only innate but also natural to produce. These types of standard or coupled reaches are different from the nonstandard reaches (Wise, di Pellegrino, & Boussaoud, 1996) that require a spatial decoupling between the action of the eyes and the hand (e.g., tool use, remote device operation). Such decoupled reach skills develop over time with experience because they require some form of training to learn the necessary reach transformation (Sergio, Gorbet, Tippett, Yan, & Neagu, 2009; Bo, Contreras-Vidal, Kagerer, & Clark, 2006; Piaget, 1965), and can be compromised by injury and neurodegeneration (Hawkins & Sergio, 2014; Salek, Anderson, & Sergio, 2011; Tippett & Sergio, 2006; Ghilardi et al., 1999).

It is well established that the core network of brain regions that support standard reaching includes the dorsal premotor cortex (PMd) and superior parietal lobule (SPL), highly interconnected regions that are part of a parietofrontal reach network (Marconi et al., 2001; Connolly, Goodale, Desouza, Menon, & Vilis, 2000; Caminiti et al., 1999; Kalaska, Sergio, & Cisek, 1998; Grafton, Fagg, Woods, & Arbib, 1996; Johnson, Ferraina, Bianchi, & Caminiti, 1996). Although studies have shown activity within PMd to be modulated by the relative position between eye and hand, the intended reach movement, wrist orientation, or hand direction (Pesaran, Nelson, & Andersen, 2006; Andersen, Musallam, & Pesaran, 2004; Raos, Umilta, Gallese, & Fogassi, 2004; Cisek & Kalaska, 2002; Boussaoud, 2001; Boussaoud & Wise, 1993), mounting evidence is growing in support of separate roles for the rostral and caudal subdivisions of PMd in visuomotor transformation (Sayegh, Hawkins, Hoffman, & Sergio, 2013; Raos et al., 2004; Picard & Strick, 2001). These results are strengthened by anatomical studies that show the vastly separate connections that PMdr and PMdc each have to frontal and parietal areas (Tanne-Gariepy, Rouiller, & Boussaoud, 2002; Petrides & Pandya, 1999; Rizzolatti, Luppino, & Matelli, 1998;

[1]York University, Toronto, Ontario, Canada, [2]Canadian Action and Perception Network, [3]University Health Network, Toronto, Ontario, Canada

doi:10.1162/jocn_a_01111

Barbas & Pandya, 1987; Matelli, Camarda, Glickstein, & Rizzolatti, 1986). Similarly, neural activity within SPL is not homogenous, and each subregion of SPL has been suggested to contribute to visually guided reaches in distinct ways (Vesia & Crawford, 2012; Breveglieri, Galletti, Gamberini, Passarelli, & Fattori, 2006; Culham & Valyear, 2006; Prado et al., 2005; Caminiti, Ferraina, & Mayer, 1998; Colby, Duhamel, & Goldberg, 1996; Mountcastle, Lynch, Georgopoulos, Sakata, & Acuna, 1975). Recent work by our group and others support these region-specific differences in the neural activity within the parietofrontal reach network during the planning and execution of different types of reaching behaviors (Granek & Sergio, 2013, 2015; Battaglia-Mayer et al., 2013; Granek, Gorbet, & Sergio, 2010; Gorbet & Sergio, 2009; Clavagnier, Prado, Kennedy, & Perenin, 2007; Prado et al., 2005; Gorbet, Staines, & Sergio, 2004; Picard & Strick, 2001; Connolly et al., 2000; Perenin & Vighetto, 1988). For example, although activity within caudal PMd and SPL regions surrounding the medial intrapareital sulcus (MIP) were enhanced during more natural coupled reaches, rostral PMd and caudal SPL showed enhanced activity for reaches that required eye–hand decoupling (Sayegh et al., 2013, 2014; Hawkins, Sayegh, Yan, Crawford, & Sergio, 2013). The overall conclusion from these studies is a separation by region of the neural responses contingent on the level of visuomotor compatibility.

Various imaging (Granek et al., 2010; Clavagnier et al., 2007; Prado et al., 2005; Gorbet et al., 2004; Connolly et al., 2000), neurophysiological (Hawkins, Sayegh, Yan, Crawford, & Sergio, 2013; Sayegh et al., 2013; Gail, Klaes, & Westendorff, 2009), and ablation or patient studies (Granek, Pisella, Blangero, Rossetti, & Sergio, 2012; Blangero et al., 2007; Kurata & Hoffman, 1994; Perenin & Vighetto, 1988; Halsband & Passingham, 1982) suggest that the cortical activity of regions, such as PMdr, PMdc, and SPL, are altered during decoupled eye–hand reaches. They concluded that, although PMd, specifically PMdr, has a stronger role in integrating a cognitive rule into the motor plan (Sayegh et al., 2013; Picard & Strick, 2001; Kurata & Hoffman, 1994; Halsband & Passingham, 1982, 1985), caudal regions within SPL may have a stronger role in the online updating and proprioceptive feedback required, principally during decoupled reach execution (Battaglia-Mayer et al., 2013; Granek & Sergio, 2013; Hawkins et al., 2013; Granek et al., 2012; Pisella et al., 2009; Blangero et al., 2007; Rossetti et al., 2005; Grea et al., 2002). It remains unclear, however, how neural activity shifts to allow for flexible visuomotor control. Although these studies support different neural circuits for the different types of visuomotor behaviors, these conclusions were made by examining the single unit or the oscillatory activity individually. To fully quantify how the brain flexibly controls different types of eye–hand compatibility, the interaction between single-unit and oscillatory activity (measured using local field potentials [LFPs]) should be examined. Specifically, we need to address how relevant these previously observed neural shifts are to the task at hand (Sayegh et al., 2013, 2014; Hawkins et al., 2013). For instance, task-relevant oscillations would need to modify the spiking activity to allow for the propagation of the task-relevant information to postsynaptic targets.

Spike–Field coherence (SFC) can measure the communication between neuronal groups that are processing task-related information and can give us an idea of how the oscillations are influencing spiking activity (Roberts et al., 2013; Vinck, Womelsdorf, Buffalo, Desimone, & Fries, 2013; Turesson, Logothetis, & Hoffman, 2012; Womelsdorf, Fries, Mitra, & Desimone, 2006; Fries, 2005). Regions exhibiting strong neuronal coherence have a greater influence over the local population and are therefore thought to promote the selection and transmission of information required to integrate sensory information for motor performance (Womelsdorf & Fries, 2006; Fries, 2005). To this end, we sought to measure the relationship between the spikes and LFPs within the subregions of PMd and SPL to determine how the coordination of neural activity changed during coupled versus decoupled reaches. Here, we demonstrate coherent activity in these regions and importantly that it is affected by the type of visuomotor mapping performed.

METHODS

Animals and Apparatus

The methods for this study have been extensively described elsewhere (Hawkins et al., 2013; Sayegh et al., 2013). Briefly, two rhesus monkeys (female *Macaca mulatta*, both 5.2 kg) were trained to perform a visually instructed, delayed reaching task in coupled and decoupled conditions. All surgical and animal handling procedures were in accordance with Canadian Council on Animal Care guidelines on the use of laboratory animals and preapproved by the York University Animal Care Committee. Each monkey was seated in front of a 38.1-cm vertical screen with an additional 38.1-cm horizontal touch-sensitive screen (Touch Controls Inc., San Diego, CA) set in front of the animal (Figure 1). The horizontal touch screen was designed to detect spatial displacements as small as 3 mm using infrared beams at a sampling rate of 100 Hz. Continuous tracking of the eye was monitored using the ISCAN-ETL 200 Eye Tracking System (ISCAN, Inc., Burlington, MA) at a sampling rate of 60 Hz.

Behavioral Task

The sequence of events is illustrated in Figure 1. Each trial began with the appearance of a red circular target (70 mm in diameter) at the center of the screen, which the monkey was instructed to touch. An additional smaller white circular target (40 mm in diameter; 5.7° of visual angle) appeared on top of the red circle, which

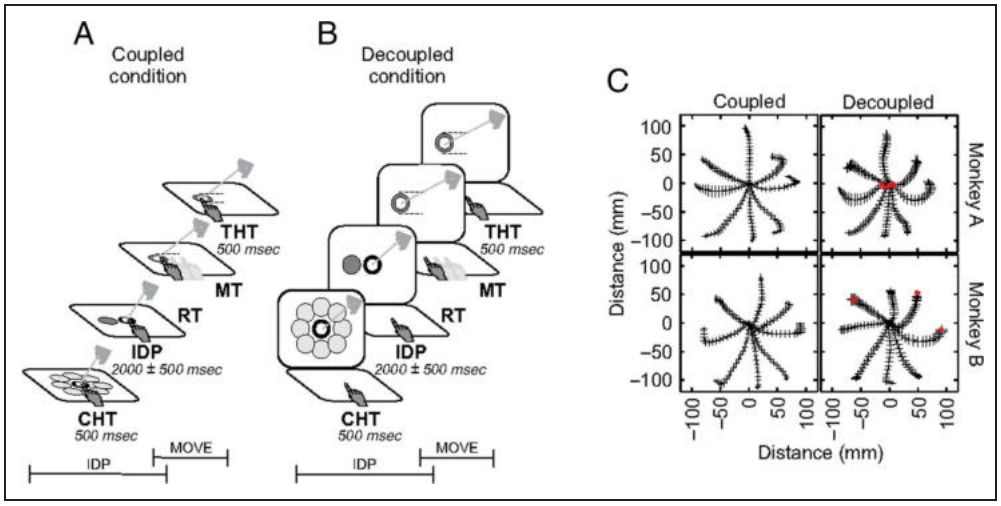

Figure 1. Experimental setup and hand trajectories for each condition. At the start of each trial, a red center target would appear with a smaller white target on top. The animal had to touch and look at these targets. After a variable delay, one of eight equally spaced (45°, light gray circles) peripheral targets was presented on either a touch-sensitive screen placed over the animal's lap (A) or on a monitor positioned vertically 40 cm away from the animal's frontal plane (B). Epochs: CHT = center hold time; IDP = instructed delay period; RT = reaction time; MT = movement time; THT = target hold time. The baseline epoch came from within the center hold time epoch. The animal's head was fixed throughout the experiment. (C) The mean reach trajectories for each monkey and condition are displayed. Black lines denote the mean movement trajectories, whereas the asterisks denote trajectory segments that were significantly more variable ($p < .05$) when compared with the standard condition.

instructed the monkey to maintain eye fixation. After a 500-msec baseline period, one of eight equally spaced green-colored peripheral targets appeared randomly (70 mm in diameter, visual angle relative to fixation). The peripheral target appeared five times at each location for a total of 40 trials per condition. After a variable instructed delay period (IDP; 2000 ± 500 msec), the red central target disappeared and the white target jumped to the peripheral target. Following this target jump, the animal moved their eyes and hand toward the peripheral target. These reaching movements were made from the middle of the center target to the middle of the peripheral target (roughly 80 mm). Once the eye and hand arrived at the peripheral target, the monkey was required to hold both the eye and the hand there for 500 msec. The visual presentation of the task was identical across conditions; however, during the eye–hand coupled condition, visual presentation and the reaching movements were both made on the horizontal touch-sensitive screen (Figure 1A). In the eye–hand decoupled condition, visual presentation of the task was on the vertical screen while the animal's limb movement remained on the horizontal touch screen (Figure 1B). This allowed us to decouple the spatial target of the eyes from that of the hand. To prevent extrafoveal tracking of the hand, an opaque screen was placed 100 mm over the animal's arm to block vision of the limb. To provide feedback on the current position of the hand, a cross-hair representing the current position of the finger on the touch screen was displayed on the vertical monitor (where the animal was looking). The animals were trained to perform similar movements during both conditions, and the biomechanical features of the movements were recorded to confirm this similarity (Hawkins et al., 2013; Sayegh et al., 2013). For each condition, two epochs during the trial were considered. The delay epoch (IDP) comprised the 500 msec baseline period and the first 2000 msec of the IDP. The perimovement epoch (MOVE) comprised the 100 msec before and first 500 msec after movement onset (8% peak hand velocity). As presented below, the 500 msec before movement onset were, on average, largely composed of the RT period (see Results).

Gaze-only Control Condition

The monkeys also performed a gaze-only control task to determine if the neural activity was affected solely by the overall shift in gaze angle. This condition has been described elsewhere (Hawkins et al., 2013; Sayegh et al., 2013). Briefly, before the start of each condition, nine white circles (40 mm in diameter; 5.7° of visual angle) appeared one at a time in the same locations as the targets that appeared during the experimental conditions (i.e., one central and eight peripheral). The monkey was instructed to fixate on each of these white circles while maintaining both hands beside the horizontal touch screen. The white circles appeared in each location three times for a total of 27 fixation points for each plane. This condition was used to determine if the oscillatory and single-unit activity within each region examined was affected solely by the overall shift in gaze angle that occurred between conditions. We recorded gaze-only data for each recording.

Neural Recordings

Monkeys were implanted with a recording cylinder under standard aseptic surgical techniques (Hawkins et al., 2013; Sayegh et al., 2013; Kalaska, Cohen, Hyde, & Prud'homme, 1989). The stereotaxic coordinates for chamber placement can be seen in Figure 2. Placement over PMd (Monkey A; Interaural A: 16 mm; L: 11 mm; Monkey B; Interaural A:

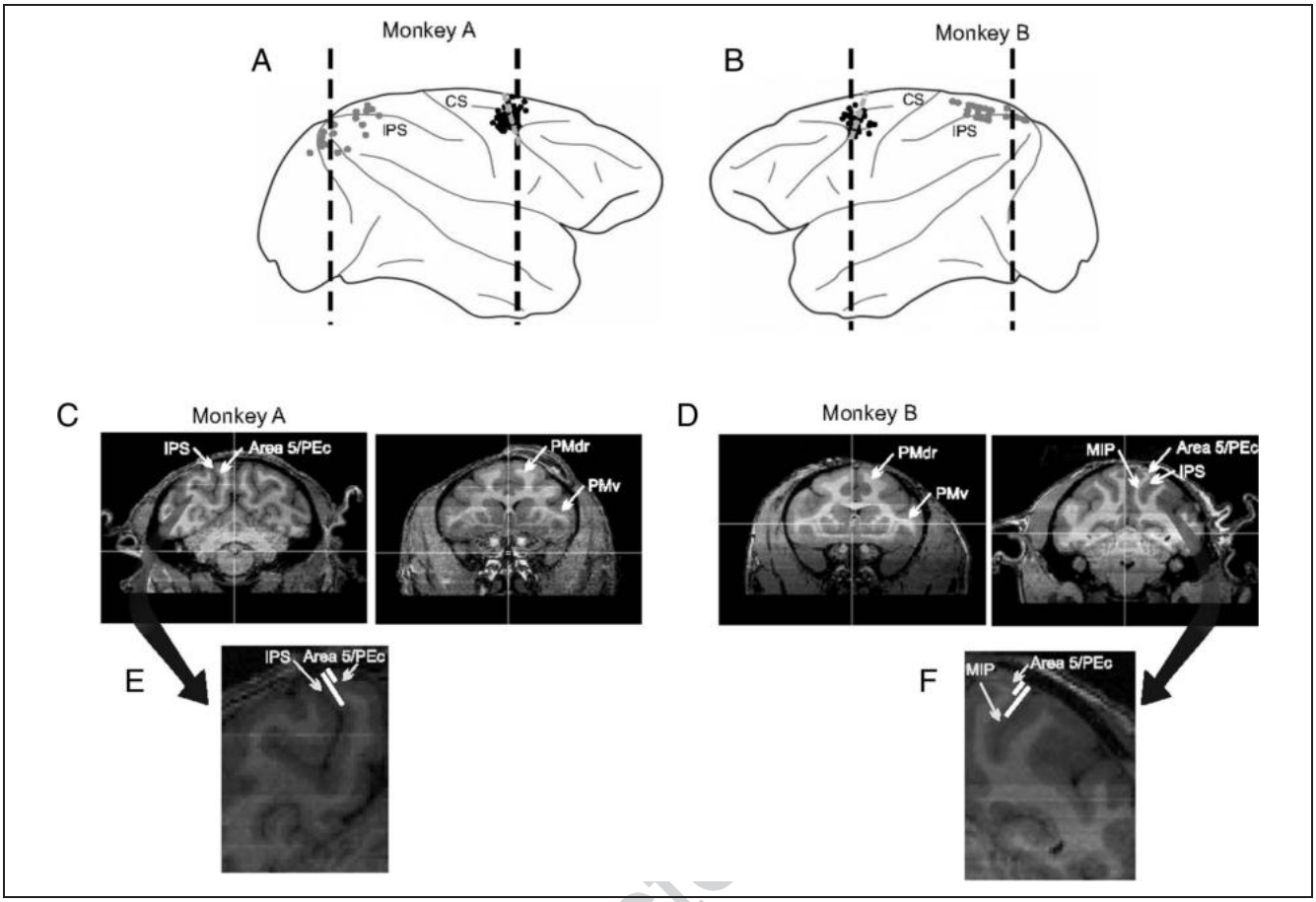

Figure 2. Penetration and chamber location sites for Monkey A (A, C and E) and Monkey B (B, D and F). Black dots represent recordings within the premotor cortex, and gray dots represent recordings within the superior parietal cortex. Larger dots indicate where recordings were obtained on two occasions, and gray dotted line denotes division between penetration sites classified as rostral or caudal dorsal premotor. (C and D) MRI slices at the level of the black vertical dotted line in A and B. (E and F) Enlarged section taken from the parietal chamber. White lines show depth information; smaller line is 2.0 mm and larger line is 5 mm to show the regions within SPL that were being recorded from based on depth. AS = arcuate sulcus; CS = central sulcus; IPS = intraparietal sulcus; PMdr = rostral region of the dorsal premotor cortex; PMdc = caudal region of dorsal premotor cortex; MIP = medial intraparietal sulcus.

16 mm; L: 11 mm) and over SPL (Monkey A, Interaural; A: −12.30 mm, L: 18.40 mm; Monkey B, Interaural; A: −7.80 mm, L: 00.00 mm) were determined using *The Rhesus Monkey Brain in Stereotaxic Coordinates* (Paxinos, Huang, & Toga, 2000). Because of the location of Monkey A's premotor chamber and a posterior head post, space limitations required the SPL chamber to be positioned on a 25° angle to allow access to the desired brain regions through deep electrode penetrations in the medial-anterior quadrant of the chamber. Thus, although the surface entry points are more rostral, the angle and depth of the electrodes provided access to neurons from within the anterior walls of the intraparietal sulcus and parietal-occipital sulci. Thus, the entry points as seen in Figure 2A and B will not give a true representation of the final location. Figure 2C–F provides a better depiction of the final location. A hydraulic multichannel driver (MCM-4, FHC, Inc., Bowdoin, ME), in conjunction with a multichannel processing system (MCP, Alpha-Omega Engineering, Israel), provided simultaneous recording from up to two penetration sites at a time. The penetrations were separated by 1–4 mm. This allowed us to examine the LFP and single units collected at each electrode site. Neural activity from each electrode was preamplified (5000×) band-pass filtered (1 Hz to 10 kHz) and split into lower (LFP) and higher (single units) frequencies. Higher-frequency signals were sampled at 12.5 kHz, and spikes of single units were sorted using template matching (Hawkins et al., 2013). The LFP (below 100 Hz) was sampled at 390.6 Hz (Sayegh et al., 2013). Following the completion of all experiments, anatomical brain images of both animals were obtained using a 3-T Siemans Magnetom Avento MRI scanner to verify chamber location (T1-weighted anatomical images, field of view = 131 × 122.8 mm, repetition time = 2300 msec, echo time = 3.54 msec, flip angle = 9°).

Data Analyses

Behavioral Analyses

To confirm that the reaching movements were biomechanically similar between conditions, hand paths were

recorded and analyzed. The results of these analyses have been extensively reported in previous papers using the same data set (Sayegh et al., 2013, 2014; Hawkins et al., 2013). In addition, to reinforce similar hand paths between conditions, movement alleys were included to ensure that reaches were directed along a fairly straight trajectory (Figure 1). These alleys were set at ±40 mm from a straight line spanning from the central to the peripheral targets. If the cursor moved outside these alleys, the trial would stop. Our comparisons confirm that the kinematic and EMG features of the limb movement between task conditions were not significantly different.

Gaze-only Control Analysis

As reported previously (Sayegh et al., 2013, 2014; Hawkins et al., 2013), LFP and single-unit activity during a gaze-only control condition. This was done in an effort to determine if the overall shift in gaze angle, which occurred between conditions, had an effect on the differences in the neural activity observed between conditions. To test the LFP activity, a subportion of the recording sites from each region was tested. For each site, the mean power (0–70 Hz) at each gaze location was calculated from a 500-msec window while the animal was fixating on the target. The mean power across all nine target locations was then computed for each condition. Bootstrapping procedures was then used to determine if any condition-related differences occurred for that site. This was repeated across all sites examined. To test for differences in the single-unit activity across the different gaze angles, a paired t test was used to compare firing rates. This was also computed for each chosen site and compared across conditions.

Spike–Field Coherence

Only task-related single units were used for this analysis. A cell was determined to be task-related if it displayed directional tuning during either the IDP or MOVE epoch. Directional tuning was determined based on previously described methods (Hawkins et al., 2013; Sayegh et al., 2013; Kalaska, Caminiti, & Georgopoulos, 1983). All LFPs that were collected simultaneously with a task-related single unit were used for analysis. Task-related PMd recordings were assigned to rostral and caudal PMd subgroups based on previously reported anatomical locations and post hoc MRI verification relative to the genu of the arcuate sulcus and can be seen in Figure 2A–D (Cisek & Kalaska, 2005; Fujii, Mushiake, & Tanji, 2000; Barbas & Pandya, 1987). Task-related SPL cells and LFPs were grouped based on depth to separate superficial (gyrus, depths < 2.5 mm past dura, defined based on average gray matter thickness) from deep (sulcus, depths > 2.5 mm past dura, generally 4–8 mm, i.e., deep enough to enter the anterior wall of the intraparietal sulcus) recordings (Figure 2E and F). Because of the location of our recordings, the superficial group is suggested to be recorded from area 5/PEc, whereas the deeper recordings are suggested to be from MIP regions. This is based on known anatomical locations and verified post hoc with MRI (Figure 2C–F).

Open source Chronux script files (www.chronux.org) were used in MATLAB (The Mathworks, Inc., Natick, MA) to analyze the spectral data and to generate time–frequency coherence plots for all spike–field pairs for both conditions (Pesaran, Pezaris, Sahani, Mitra, & Andersen, 2002; Jarvis & Mitra, 2001). SFC was determined using multitaper spectrum analysis (previously described in Pesaran, Nelson, & Andersen, 2008; Pesaran et al., 2002; Jarvis & Mitra, 2001), using a time-bandwidth product of TW = 5 with K = 9 tapers and a 500-msec window. The coherence was then transformed using the assumption that when the coherence is zero, the transformed coherence is distributed as a normal variate with the variance equal to 1 (Pesaran et al., 2002; Jarvis & Mitra, 2001). Target direction was collapsed so that coherence estimates represent the overall SFC for each condition regardless of hand movement direction. The population coherence was then determined, and task-related differences were then determined using bootstrapping procedures (Hawkins et al., 2013; Sayegh et al., 2013). Because some spike–field pairs were recorded on the same electrode, we compared the results obtained from these pairs to spike–field pairs from different electrodes. The same pattern of coherence results were observed between groups, and thus, the population results represent both groups. Lastly, the labels assigned to frequency ranges are, to put it mildly, heterogeneous across the nonhuman primate literature. To maintain consistency with our previous work, we refer to activity with oscillations in the 6–15 Hz range as alpha-band, 16–30 Hz as beta-band, and 31–70 Hz as gamma-band. We recognize that some studies refer to the lower end of our alpha-band as belonging within the theta-band range.

Further, we were not able to calculate SFC measures across the different regions examined. Because of technical constraints, we were not able to record simultaneously from PMd and SPL. Although we feel that this is a limitation of the study, the results we obtained from the local SFC enriches and supports the understanding of how the local processing within these regions change as a function of eye–hand coupling.

Meta-analysis

Inclusion Criteria

The cell recording data presented here indicate that, within the macaque brain, functional activity associated with standard and nonstandard visuomotor transformations localizes to different but contiguous and overlapping regions of the dorsal premotor and superior parietal cortices. To examine whether or not the literature contains evidence of a similar spatial distribution

of activity in the human brain, we performed a quantitative meta-analysis of published imaging data. Studies that were included in the meta-analysis used functional imaging to examine brain activity associated with standard and/or nonstandard visually guided arm movements. A study was considered to have examined a standard visuomotor mapping when participants were required to initiate spatially and temporally congruent eye and hand movements to the same target location. Note that the hand movement had to consist of a direct interaction with the target. Nonstandard visuomotor mappings were defined as any condition in which the eye and hand went to spatially noncongruent target locations (e.g., joystick use, eye and hand movements made in different directions, hand movement with eye fixation, etc.). Regions activated by observed or imagined movements were not included. Within each of the selected studies, an area of reported activation was included in the meta-analysis if it was within either the PMd or the SPL. The Talairach coordinate boundaries of the PMd were defined according to Mayka, Corcos, Leurgans, and Vaillancourt (2006). The boundaries of the SPL were defined so that an area was

Table 1. The Studies Selected for Inclusion into the Coupled Reach Condition

Author, Year	*N (f)*	*Task*	*PMd Coordinates*	*SPL Coordinates*
Desmurget et al., 2001	7	Look and point task – look only task	−41 −23 62	−27 −54 59
				−24 −63 51
Filimon, Rieth, Sereno, & Cottrell, 2014	16	Direct foveated reaching		8 −67 52
				−29 −55 54
				−15 −77 43
Hinkley, Nagarajan, Dalal, Guggisberg, & Disbrow, 2011	8	Direct foveated reaching	−39 −2 57	−30 −60 65
				25 −60 65
				−35 −40 65
Gallivan, McLean, Smith, & Culham, 2011	8	Direct foveated grasp – visual presentation	−28 −14 53	
			26 −14 51	
Gorbet et al., 2004	10	Direct foveated hand movement > decoupled reaching	−26 −17 54	27 −41 59
			−33 −17 54	
			8 3 54	
			20 −6 65	
Gorbet & Sergio, 2007	20	Standard reaching – central fixation	35 −8 59	27 −42 60
Granek, unpublished data	10	Direct foveated reach – central fixation	−49 −17 43	−15 −56 42
				−18 −60 35
				−5 −69 31
Prado et al., 2005	12	Direct foveated reach – saccade task	−38 −22 53	−30 −47 61
			36 −11 47	34 −48 61
Singhal, Monaco, Kaufman, & Culham, 2013	11	Direct foveated reach	−28 −13 55	−27 −55 45
			23 −9 49	25 −51 45
			−25 −18 63	12 −73 43
			24 −13 61	20 −70 36
				3 −70 43
				30 −51 56
				6 −72 45
				4 −60 52
				3 −50 58

Table 2. The Studies Selected for Inclusion into the Decoupled Reach Condition

Author, Year	*N (f)*	*Task*	*PMd Coordinates*	*SPL Coordinates*
Beurze, Toni, Pisella, & Medendorp, 2010	14	Nonfoveal reaching	−24 −13 58	−24 −52 58
			25 −10 58	24 −51 58
			−26 −13 63	−22 −63 49
			21 −13 70	22 −64 49
Fabbri, Caramazza, & Lingnau, 2010	14	Nonstandard plane change – baseline	−21 −9 56	27 −45 46
			20 −11 54	−19 −61 51
				11 −64 47
Fabbri, Strnad, Caramazza, & Lingnau, 2014	16	Instruct on screen, reaches to sphere on chest no visual feedback	−33 −22 56	−17 −56 55
Filimon, Nelson, Hagler, & Sereno, 2007	16	Extra-foveal reach – baseline	−23 −17 55	−26 −56 58
			33 −15 60	17 −60 57
			−21 −6 60	
			20 −10 63	
			−31 −2 61	
Filimon, Nelson, Huang, & Sereno, 2009	20	Extra-foveal reach > saccade only		−9 −54 60
				11 −54 58
Gorbet et al., 2004	10	Decoupled reach > direct foveated reach	11 17 63	21 −44 62
			38 15 41	20 −4 62
			23 −5 63	
Gorbet & Sergio, 2007	20	Decoupled reach – central fixation		23 53 −50
				30 −45 60
				26 −59 58
Grafton, Hazeltine, & Ivry, 1998	10	Conditional movement – (power and precision movement)	−33 −3 48	−13 −63 49
Granek et al., 2010	10	Rotated reaching movement – central fixation	−6 14 60	11 −68 41
			30 −6 67	−9 −58 33
			30 12 47	4 −62 31
				−16 −52 38
				−14 −60 39
Haaland, Elsinger, Mayer, Durgerian, & Rao, 2004	14	Sequence of button presses, cue on screen button not visible	−24 −7 47	−26 −56 43
				26 −64 39
Kertzman, Schwarz, Zeffiro, & Hallett, 1997	20	Extrafoveal reach	−24 −12 60	−18 −60 56
Prado et al., 2005	20	Extrafoveal reach – saccade task	−34 −11 43	−32 −40 61
			26 −14 63	−16 −74 44
			8 −3 63	−22 −52 66
				30 −53 58

Table 2. (*continued*)

Author, Year	*N (f)*	*Task*	*PMd Coordinates*	*SPL Coordinates*
Thoenissen, Zilles, & Toni, 2002	6	Intention of a conditional finger movement task (go > no-go)	−10 8 60	
Toni et al., 2002	6	Conditional finger movement task	−26 −2 54	10 −74 46
			−48 4 40	−26 −56 62
			−38 −14 56	36 −54 54
			−26 −20 68	−30 −68 52
			−14 8 70	−18 −70 52
			−38 −14 64	−12 −58 70
			−42 −8 54	−4 −74 48
			−48 4 42	8 −74 48
			44 −12 62	−26 −56 62
				−30 −62 46
				−8 −76 56
				−18 −70 52
Tunik, Saleh, & Adamovich, 2013	12	Nonstandard finger movement > standard finger movement	−40 −20 68	−22 −54 54
			−36 4 50	
			−58 −18 42	

included if it was within either Brodmann's area 5 or 7 according to the Talairach Daemon (Lancaster et al., 2000; www.talairach.org). Tables 1 and 2 contain a list of studies that were included in the meta-analysis. In total, 23 studies were included with 55 PMd foci and 72 SPL foci.

Activation Likelihood Estimation Analysis

An activation likelihood estimation (ALE) analysis was used to determine the probabilistic distribution of activation and peak coordinates of activity within the PMd and SPL across the selected studies (Laird et al., 2005; Turkeltaub, Eden, Jones, & Zeffiro, 2002). The analysis was performed using GingerALE 2.3 (Turkeltaub et al., 2012; Eickhoff et al., 2009; https://brainmap.org/ale/). This method of meta-analysis takes the number of participants in a study into consideration by altering the Gaussian function used to smooth each region included in the analysis so that a larger number of subjects gives a region more weight (Eickhoff et al., 2009). Foci were analyzed in Talairach space. Foci originally reported in MNI space in any of the included studies were converted to Talairach space for the meta-analysis. ALE scores were calculated separately for standard and nonstandard foci using false discovery rate (FDR pN) correction for multiple comparisons with a threshold set to $p < .01$ and minimum cluster size set at 100 mm^3. Resulting thresholded ALE scores were contrasted to test for statistically significant differences in spacial convergence. A conjunction image was also created to show where the two data sets (i.e., standard and nonstandard foci) overlap. Visualization of the results used Mango software (ric.uthscsa.edu/mango/mango.html) with a Talairach template underlay (available from https://brainmap.org/ale/).

RESULTS

Behavioral Results

As a first step, we analyzed the biomechanical features of the reaches performed in each condition. This was to ensure that differences that occurred in the neural activity between tasks were not a direct result from differences in the reach profile. The results of these analyses have been extensively reported previously (Sayegh et al., 2013, 2014; Hawkins et al., 2013). Briefly, when comparing between conditions, we observed no significant differences in the variability of the reach trajectories ($p > .05$), in the reach velocity ($p > .05$), in the RTs (coupled: $M = 537.9$ msec, $SEM = 12.82$; decoupled: $M = 522$ msec, $SEM = 9.89$), or in the EMG data ($p > .01$). Taken collectively, our comparisons confirm that the kinematics and EMG features of the limb movement

between conditions were not significantly different. Therefore, any task-related difference observed within this study can be interpreted as due to differences in the processing of the motor behavior.

Gaze-only Control Results

As previously stated (Sayegh et al., 2013, 2014; Hawkins et al., 2013), the overall shift in gaze angle was not a sole contributor of the differences in neural activity between conditions for each region examined. We observed no significant difference in the neural activity (LFPs and single units) when comparing between conditions during the gaze-only control task ($p > .05$). Therefore, we can interpret the task-related differences in the neural data as being due to rule-processing rather than solely to a shift in gaze angle.

Neural Results

To investigate the coordination between spiking activity and LFP activity during visually guided reaching movements, we recorded the activity of 207 spike–field pairs (39 within PMdr, 30 within PMdc, 77 within PEc, and 61 within MIP). All spike–field pairs were used for the statistical analyses for each region. SFC measures the relationship of the spiking neurons to the LFP (Pesaran et al., 2008; Womelsdorf & Fries, 2006), and thus, it is an appropriate measure to gain insight into the computations of each of these region to different types of visually guiding reaching movements. Overall significant SFC occurred within the planning of visually guided reaching movements (Figures 3 and 5). However, consistent with our previous reports (Sayegh et al., 2013, 2014; Hawkins et al., 2013), we saw region-specific differences in the neural responses based on the type of reach being

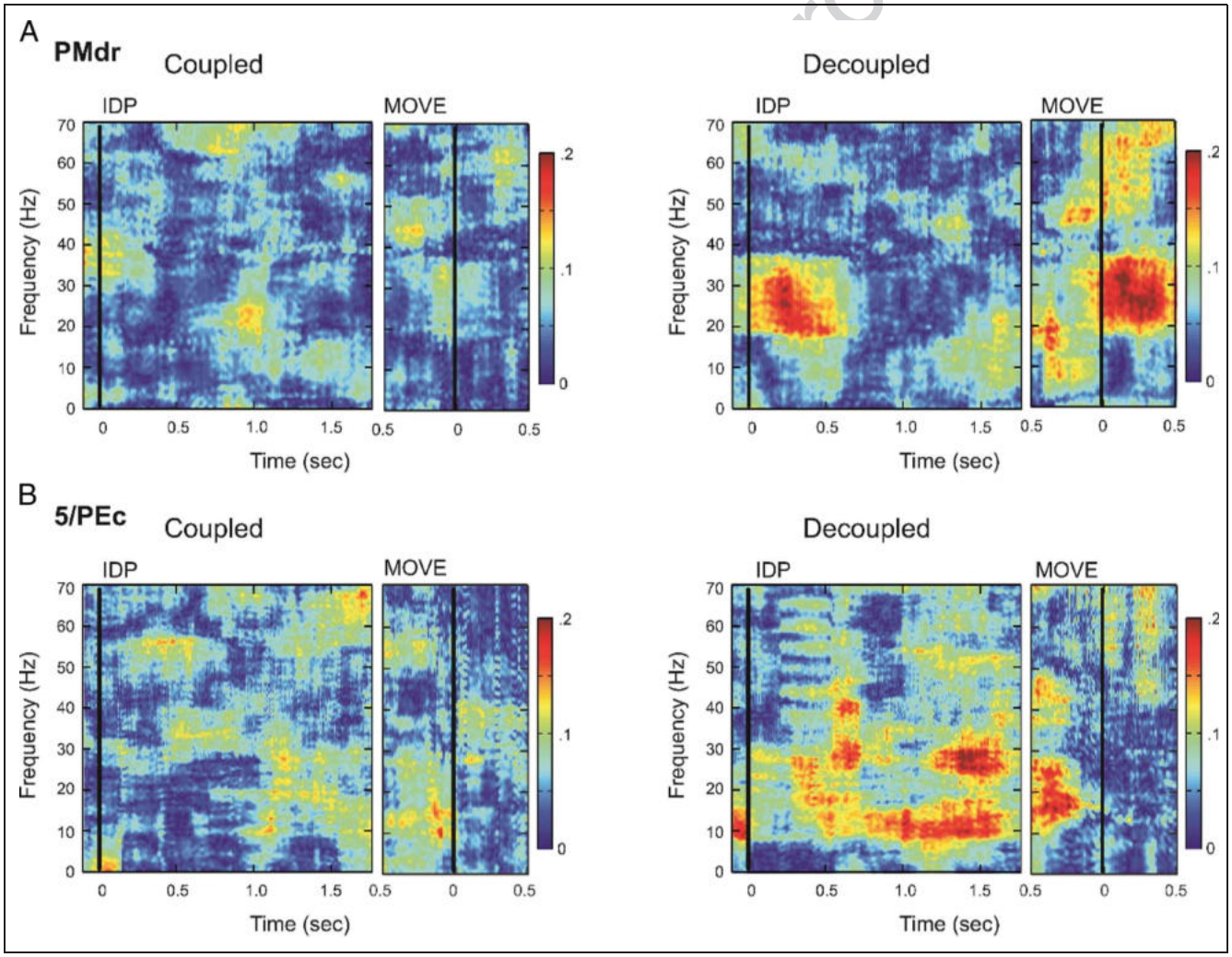

Figure 3. Example of SFC. (A) An example site from PMdr during IDP epoch and MOVE epochs for both conditions. (B) PEc example during IDP epoch and MOVE epochs for both conditions. Results show a different pattern of coherence for each region examined. Results were aligned to peripheral cue onset (during IDP epoch) and to movement onset (during MOVE epoch), represented by the black vertical line. Amplitude is color coded.

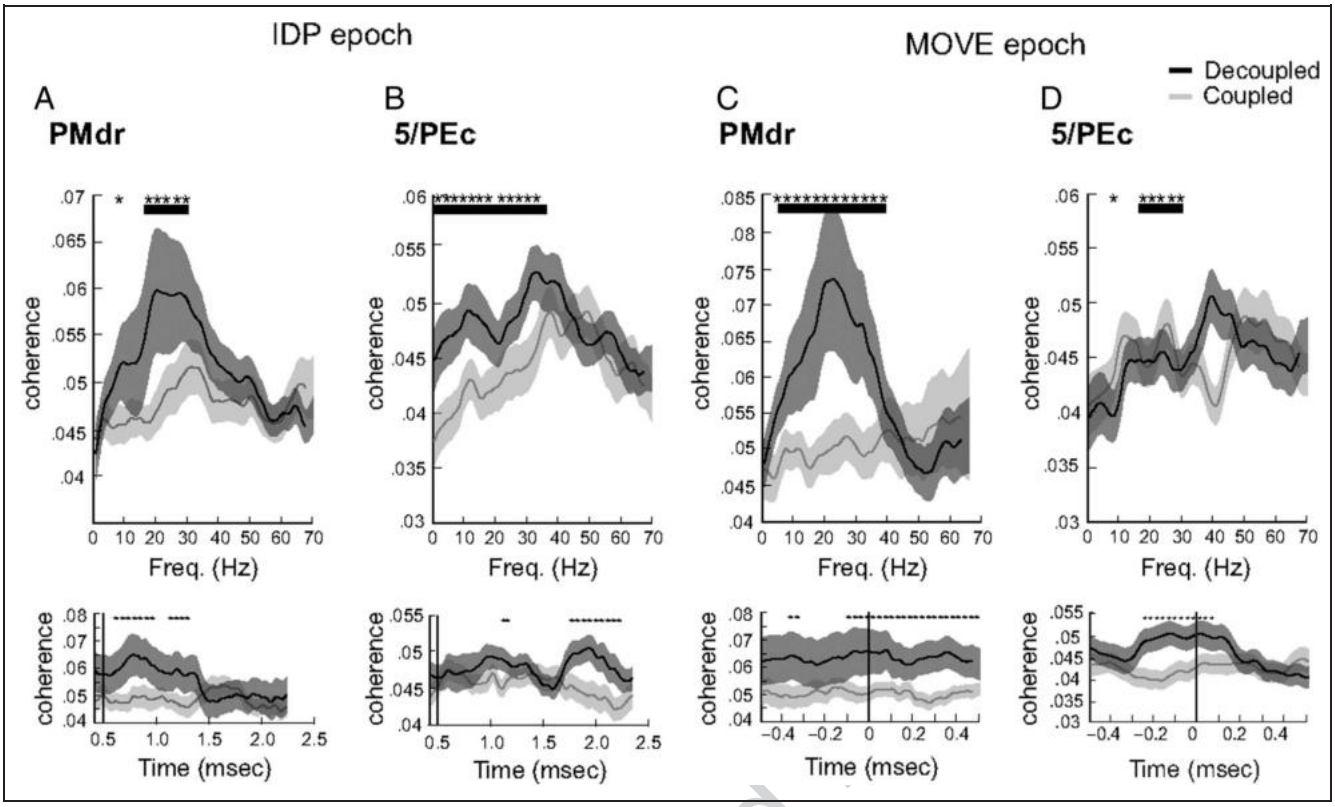

Figure 4. SFC across the population of PMdr and PEc sites. (A and B) Raw coherence plots during coupled (gray) and decoupled (black) conditions during IDP epoch for PMdr (A) and PEc (B) regions. Top plots represent the average population coherence values across the frequencies examined. Bottom plots represent the characteristics of the SFC across the population over time. (C and D) Raw coherence plots during MOVE epoch for PMdr (C) and PEc (D) epochs. Top plots represent the average population coherence values across the frequencies examined. Bottom plots show the characteristics of the SFC across the population over time. Asterisks denote significant difference between conditions $p < .05$. Black horizontal bar shows analysis window bottom plots.

performed. More specifically, we observed an enhancement in the SFC across the population of recordings within PMdr and 5/PEc for decoupled when compared with coupled reaches (Figures 3–5) whereas PMdc and MIP displayed enhanced SFC during coupled reach conditions (Figures 6–7).

Stronger SFC during Decoupled Reaches

PMdr and 5/PEc were regions that showed a consistent enhancement in SFC when the reach condition required a spatial decoupling between the final gaze and hand motion targets (Figure 3). The neural response within PMdr displayed task-related SFC differences within the lower (10 Hz) and higher (17–35 Hz) frequency range during the planning of a decoupled reach (Figure 4A, top, $p <$ .05). When examining the time course of these differences, these task-related differences emerged roughly 100 msec after the peripheral cue onset (Figure 4A, bottom, $p < .05$). Within 5/PEc, we observed a similar pattern of results across the population (Figure 4B). A strong SFC was observed within a lower (0–20 Hz) and slightly higher range (25–38 Hz) for decoupled versus coupled reach planning (Figure 4B, top, $p < .05$). These task-related coherence differences also emerged following the cue onset. These differences occurred both early (~1000 msec) and late (~1600 msec) within the planning epoch (Figure 4B, bottom, $p < .05$).

As the trial progressed to the execution phase of the movement, PMdr and 5/PEc remained as the two regions that displayed the strongest SFC during decoupled versus coupled reaches (Figure 3). Across the population, PMdr demonstrated significantly greater SFC within the 5–40 Hz range for decoupled when compared with coupled reach execution (Figure 4C, top, $p < .05$). These taskrelated coherence differences began during the late RT and remained significantly different between conditions following movement onset (Figure 4C, bottom, $p < .05$). Within 5/PEc, enhanced SFC occurred for decoupled reaches within the 40–50 Hz range (Figure 4D, top, $p < .05$), emerging roughly 300 msec before the onset reach execution (Figure 4D, bottom, $p < .05$).

In summary, decoupled reaches were associated with enhanced synchrony within PMdr and 5/PEc relative to reaches involving direct object interaction. PMdr and PEc displayed strong alpha- and beta-band SFC beginning shortly after the onset of the peripheral cue. By reach execution, the task-related enhancements in SFC within

PMdr and 5/PEc occurred in higher beta- and gamma-bands. Taken collectively, these results suggest that PMdr and 5/PEc preferentially process the visuomotor transformations necessary during decoupled eye–hand reaches.

Stronger SFC during Coupled Reaches

Contrary to the observations of PMdr and 5/PEc activity described in the above section, SFC within PMdc and MIP were significantly stronger during the performance of a coupled reach when compared with a decoupled reach (Figure 5). Across the population of recordings, during coupled reach planning PMdc displayed stronger SFC within the 5–20 Hz range than when compared with decoupled reach planning (Figure 6A, top, $p < .05$). When observing the time course of these differences, they emerged roughly 2000 msec after the peripheral cue was displayed (Figure 6A, bottom, $p < .05$).

Unlike PMdc, MIP showed no task-related SFC differences for coupled versus decoupled reach planning (Figure 6B, $p > .05$). By reach execution, the previously observed task-related differences within PMdc also disappeared (Figure 6C, top, $p > .05$). However, MIP displayed a stronger SFC for coupled when compared with decoupled reaches (Figure 6D, top, $p < .05$). More specifically, stronger SFC was observed in MIP within the 50–60 Hz range (Figure 6D, top, $p < .05$) occurring shortly after the onset of the reaching movement (Figure 6D, bottom, $p < .05$). Taken collectively, PMdc and the MIP demonstrate enhanced synchrony for coupled when compared with decoupled reaches. PMdc demonstrated enhanced alpha and beta band SFC during the planning of coupled reaches that resolved by movement onset. MIP showed stronger gamma band synchrony during the execution of coupled reaches. These results suggest that, during the control of coupled reach, there is enhanced local communication within PMdc and MIP, supporting a stronger role of these regions in coupled visuomotor transformations.

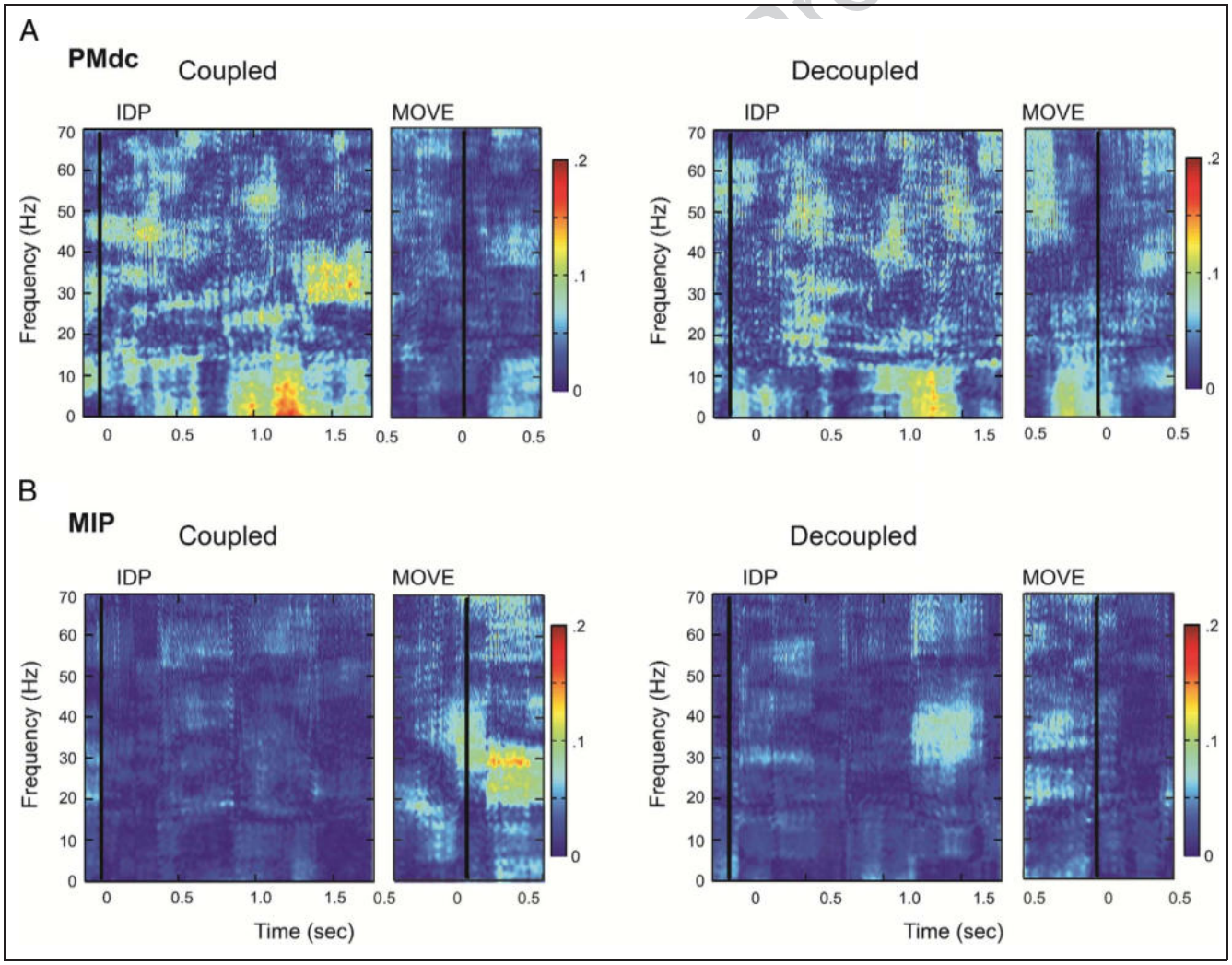

Figure 5. Example of SFC. (A) PMdc example site during IDP epoch and MOVE epoch. (B) Example site from PEc during IDP epoch and MOVE epochs. Results show a different pattern of coherence for each region examined. Results were aligned to peripheral cue onset (during IDP epoch) and to movement onset (for MOVE epoch), represented by the black vertical line. Amplitude is color coded.

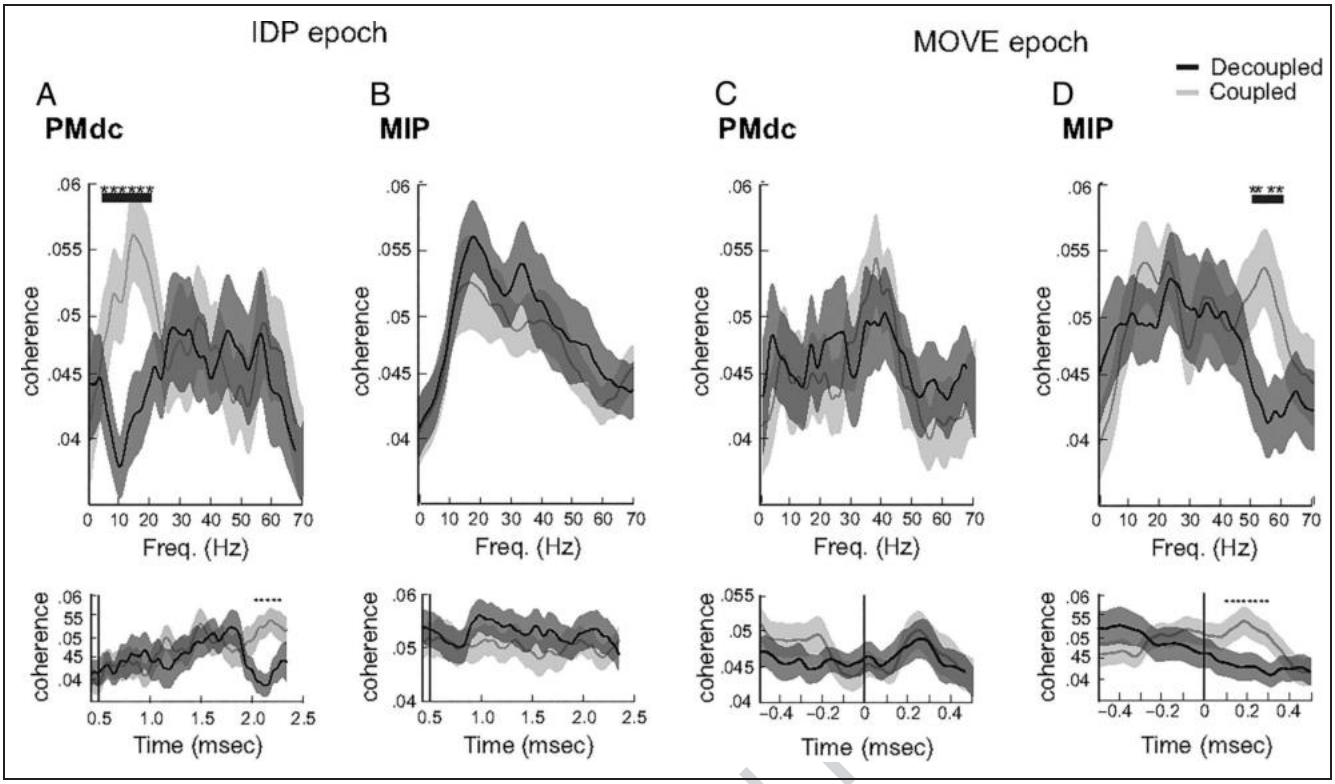

Figure 6. SFC across the population of PMdc and MIP sites. Figure setup is the same as in Figure 4.

Meta-analysis Results

ALE meta-analyses were performed to compare patterns of functional activity associated with standard visuomotor mappings versus nonstandard mappings. The results of the ALE analyses demonstrate that functional activity evoked by decoupled eye–hand mappings relative to coupled mappings are significantly more rostral/medial in the left PMd and more caudal/medial bilaterally in the SPL. However, conjunction meta-analyses demonstrate that there is a significant region of overlap for the two types of mappings in both the PMd and SPL regions, suggesting a gradient of task-specific functional activity in these areas. These findings are visualized in Figure 7, and the Talairach coordinates of regions showing significant differences between the two types of visuomotor mappings are given in Table 3.

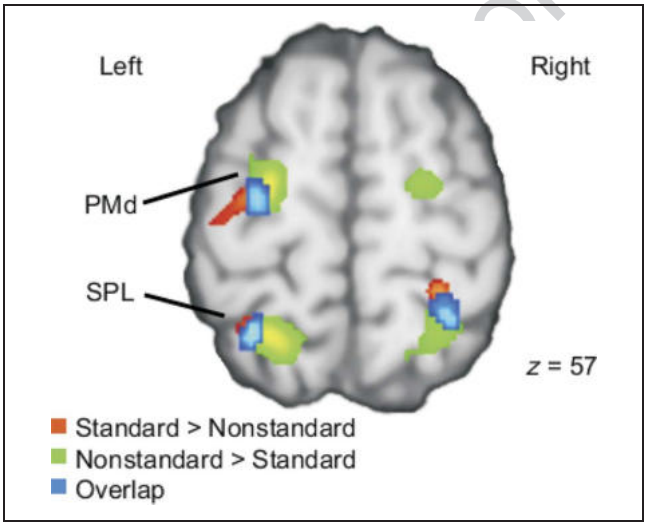

Figure 7. Results of ALE meta-analyses. Results are overlaid on an axial slice from a Talairach anatomical template at $z = 57$. Orange regions are significantly more likely to be active during coupled eye–hand visuomotor mapping tasks relative to decoupled visuomotor mapping tasks. Green regions are significantly more likely to be active during decoupled tasks relative to coupled tasks. Blue regions represent areas with significant amounts of overlap, indicating activity during both types of mappings.

DISCUSSION

Decoupled visually guided reaches require additional processing in a number of ways compared with coupled reaching movements. First, decoupling the spatial target of the eyes from the hand requires a greater cognitive influence over the sensory to motor transformation. For instance, a rule regarding the spatial transformation obetween the eyes and the hand must be incorporated into the upcoming reach plan. Second, because of the natural tendency for the action of the eyes and the hand to move together (Terao, Andersson, Flanagan, & Johansson, 2002; Henriques, Klier, Smith, Lowy, & Crawford, 1998; Sergio & Scott, 1998; Vercher, Magenes, Prablanc, & Gauthier, 1994; Gauthier & Mussa Ivaldi, 1988), the computations involved in decoupled reaching must account

Table 3. Comparison of the Spatial Patterns of Functional Activity during Standard and Non-standard Mappings

Brain Area	*Talairach Coordinates*	*Size (mm^3)*
Standard > Non-standard		
Left PMd	−28, −14, 54	1397
Left SPL	−28, −54, 56	501
Right SPL	28, −42, 60	657
Non-standard > Standard		
Left PMd	−22, −10, 58	1819
Right PMd	24, −10, 62	1454
Left SPL	−18, −58, 54	2783
Right SPL	28, −54, 58	802
Right SPL	12, −66, 44	105
Overlap		
Left PMd	−26, −14, 56	643
Left SPL	−28, −54, 56	623
Right SPL	28, −46, 60	573

PMd = dorsal premotor cortex; SPL = superior parietal lobule.

for disengaging this linkage (Sergio et al., 2009; Murray, Bussey, & Wise, 2000; Wise et al., 1996). Finally, incongruent visual and sensory information will result in unreliable visual signals regarding the position of the hand relative to the target. Thus, hand position must be derived predominantly from proprioceptive feedback and efference copy information (Buneo & Andersen, 2006; Engel, Flanders, & Soechting, 2002; Rushworth, Nixon, & Passingham, 1997; Flanders, Helms-Tillery, & Soechting, 1992). This extra processing is incorporated into the reach-related signal for successful performance. Although PMd and SPL are well-established players in reaching related activity, the weight of these regions and, in particular, their subregions will not be homogenous to the various types of visuomotor transformation. For instance, PMdr is strongly interconnected with the pFC (Tachibana, Nambu, Hatanaka, Miyachi, & Takada, 2004; Lu, Preston, & Strick, 1994) and has been hypothesized to have a more cognitive or high-order influence over reach-related activity, specifically when a reach relies on a rule to dictate the relationship between the eyes and the hand (Sayegh et al., 2013; Abe & Hanakawa, 2009; Picard & Strick, 2001). On the contrary, PMdc is more directly connected to the primary motor system (M1), preferentially coding limb movement parameters (Cisek, Crammond, & Kalaska, 2003; Alexander & Crutcher, 1990; Kurata, 1989) primarily when arm movements are controlled by visual or somatosensory information (Abe & Hanakawa, 2009; Luppino, Rozzi, Calzavara, & Matelli, 2003). Similar divisions are present within SPL. MIP is involved in the planning and execution of goal-directed reaches (Colby, 1998) and its activity is thought to reflect the online automatic corrections of coupled reaches (Clavagnier et al., 2007; Prado et al., 2005), whereas area PEc houses somatosensory cells, which are responsible for limb monitoring and maintaining an updated relative position of ones' body (Breveglieri et al., 2006; Mountcastle et al., 1975). Taken collectively, one can expect variability within the neural activity across these PMd and SPL regions contingent on the type of visuomotor transformation at hand. This is indeed what we observed; depending on the region examined, we observed changes to the spike–field relationship that was influenced by the type of eye–hand coordination performed. To our knowledge, we are the first group to show these task-dependent changes in SFC.

The Spike–Field Relationship

The relationship of the spiking activity to the LFPs is an important relationship to examine when trying to understand how a region is selecting and transmitting information required to integrate sensory information for motor performance (Womelsdorf & Fries, 2006; Fries, 2005). Oscillatory activity can produce fluctuations in the intracellular potential of targeted postsynaptic neurons, generating temporal windows of communication between these two assemblies (Ray, 2015; Buzsaki, Anastassiou, & Koch, 2012; Bartos, Vida, & Jonas, 2007). Action potentials that are coupled, at the opportune time, within this window have a greater chance of eliciting downstream targets (Womelsdorf et al., 2007).

The importance of this spike–field interaction was evident when comparing our results across studies. For instance, although previous work reported a significant difference in alpha band activity within PMdr between identical task conditions, no difference was observed in the spiking activity (Sayegh et al., 2013). Recently, Gorbet et al. (2016) used fMRI to examine human brain activity associated with coupled versus decoupled reaches. Surprisingly, they did not observe differences in the activation of many of the key reach-related regions when contrasting between reach types (Gorbet & Sergio, 2016). Although this may seem surprising, these results highlight the importance of considering local communication within a region and how it may change when trying to understand how a region encodes different types of behaviors. These findings suggest that a key factor for the flexible processing within a region to account for task-specific requirements is the timing of spiking activity and not solely the spike rate for information processing (Saalmann, Pigarev, & Vidyasagar, 2007; Womelsdorf & Fries, 2006; Fries, 2005). The synchronization of activity, specifically at different frequency bands, may be a reliable way for a region to engage cortical circuits to coordinate task-related processes (Wu, Wheeler, Staedtler, Munk, &

Pipa, 2008). More specifically, this timing would be critical between reciprocally connected frontoparietal regions because it would identify and select neuronal pools based on the arrival of action potentials (Battaglia-Mayer, Ferrari-Toniolo, & Visco-Comandini, 2015). These neuronal pools could simultaneously represent various sensorimotor representations of the reach signal, allowing for flexible control and representation within the brain (Battaglia-Mayer et al., 2015).

PMdr and 5/PEc Preferentially Process Decoupled Reaches

Of the examined regions, PMdr and area 5/PEC consistently showed enhanced SFC for decoupled when compared with coupled reaches. More specifically, area 5/PEc and PMdr both showed enhanced alpha-band SFC within the planning of decoupled reaches. Alpha-band synchrony has been observed to dominate during the active inhibition of a not-to-be-applied rule (Buschman, Denovellis, Diogo, Bullock, & Miller, 2012). During decoupled reach planning, an inhibitory signal must be present to allow for the dissociation between the eyes and the hand. Additional research here, such as muscimol studies targeting PMdr, would be an elegant way of examining the importance of alpha band synchrony to decoupled reach planning.

Progressing from planning into movement, we observed stronger beta-band SFC within both PMdr. SFC within the beta band range has been shown to dominate within the infragranular cortical layers where many feedback projections terminate, an arrangement indicative of top–down control (Bastos et al., 2012; Bosman et al., 2012; Spaak, Bonnefond, Maier, Leopold, & Jensen, 2012; Engel & Fries, 2010; Maier, Adams, Aura, & Leopold, 2010). Importantly, beta-band activity is thought to be involved in the high-order executive function of rule selection within the pFC (Buschman et al., 2012). PMdr and the dorsolateral pFC have been shown to become functionally coupled when a motor behavior is guided by a rule (Abe & Hanakawa, 2009; Luppino et al., 2003; Murray et al., 2000), and thus, it is possible that the strong synchronization of the spikes and LFPs at the beta-band range reflects the integration of the spatial rule into the motor plan. Furthermore, long-range beta-band synchronization mediates top–down processing (Buschman & Miller, 2007) between regions. The present data support the notion that PMdr is communicating the rule-updated motor plan to other reach-related regions.

During movement, the incongruent eye and hand signals require online processing in regions of SPL, such as 5/PEc, where proprioceptive feedback is integrated into the ongoing motor command to monitor limb position and update body position (Jackson et al., 2009; Buneo & Andersen, 2006; Rushworth et al., 1997). Around the time of movement onset, we observed strong gamma-band synchronization between the spikes and LFPs within area 5/PEc. Neuronal synchrony and coherence within the gamma-band range is observed within the superficial and granular cortical layers of a region, indicative of "bottom–up" or feed-forward processing (Bastos et al., 2012; Bosman et al., 2012; Maier et al., 2010). One possibility is that this enhanced gamma SFC could represent or provide the extra proprioceptive and efference copy signals needed to perform a decoupled reach to SPL. Similarly, the observed gamma-band synchrony within PMdr could reflect online error correction during the remapping of the relative position of the arm to the eyes (Lee & van Donkelaar, 2006; Pesaran et al., 2006; Caminiti, Johnson, Galli, Ferraina, & Burnod, 1991). It would be worth exploring the idea that the early alpha and beta signals within PMdr and 5/PEc reflect rule integration and inhibition of eye–hand coupling. Similarly, by reach onset the local computation could shift to reflect the enhanced proprioceptive control needed during decoupled reach execution.

PMdc and MIP Preferentially Process Coupled Reaches

Contrary to our abovementioned results, we observed stronger SFC for coupled reaches within PMdc and MIP. This is not surprising when considering PMdc's direct connection to the primary motor cortex, coding limb movement parameters when arm movements are controlled by visual or somatosensory information (Gail et al., 2009; Lee & van Donkelaar, 2006; Prado et al., 2005; Picard & Strick, 2001). Similar observations were made for regions in the medial intraparietal sulcus within SPL (Colby, 1998), thought to have a more active role in the online automatic corrections of coupled reaching movements (Clavagnier et al., 2007; Prado et al., 2005). For instance, we observed relatively greater SFC in MIP within the gamma-band range during the coupled reach, an action requiring little cognitive control. Because gamma-band synchrony is indicative of bottom–up processing (Bastos et al., 2012; Bosman et al., 2012; Maier et al., 2010), the observed enhancements in gamma-band SFC during coupled reaches could reflect the local biomechanical computations required to perform a simple reaching task.

By reach execution, the task-related difference observed within PMdc during reach planning resolved. In conjunction with the similarity in reach profiles between conditions, this implies that PMdc is not affected by the type of visuomotor transformation being executed. However, if this was true, then we would expect no difference to occur in the planning of coupled versus decoupled reaches, which was not the case. PMdc is affected by the compatibility between the eyes and the hand with less weight placed on PMdc for computing the necessary visuomotor transformation during decoupled reaches. Whether these regions are inhibited or the activity of regions such as PMdr and PEc supersede them remains to be determined. In recent support of our findings, Stetson

and Andersen (2014) found that the SFC activity between PMd and "PRR" (likely PMdc and MIP based on reported recording locations) were anticorrelated during extrafoveal reaching tasks, suggesting that communication between these regions was suppressed during this type of reach (Stetson & Andersen, 2014). This suppression may be necessary to allow for other reach regions, such as PMdr and 5/PEc, to process the more complicated transformation.

It is important to note that, despite the evidence of a functional separation between PMdr, PMdc, and regions of SPL (PEc versus MIP) in visuomotor control, each of these regions were active for both types of tasks. Abe et al. (2009) recently suggested that, depending on the coupling of PMd to other regions, PMd can operate in a top–down or bottom–up fashion (Abe & Hanakawa, 2009). We extend these conclusions and suggest that during more natural coupled reaches all of these regions may engage in bottom–up types of processing by responding to the visual and somatosensory inputs received by the system. In fact, we previously observed no major difference in the spectral profile between PMdr and PMdc during coupled reaching (Sayegh et al., 2013). However, when a rule is needed to guide behavior, the communication of PMdr with dorsolateral pFC and regions of SPL, such as PEC, may allow for such top–down processing like rule integration. Future studies examining the coupling between these regions during different types of visuomotor compatibilities would be of interest. A major disadvantage of this study was that no simultaneous recordings between PMd and SPL were recorded. Thus, future work designed to address these questions will need to obtain simultaneous recording between these regions to fully characterize the communication differences that may results from changing the coupling of the eye to the hand.

Region-related Changes during Different Mappings in Humans

Our work supports the idea of altered cortical control during different types of visuomotor mappings and highlights the need to account for the decoupled nature of a motor task when interpreting movement control research. Our meta-analysis of fMRI findings provides evidence of a similar functional topography in which there is a delineation in the cortical activity of coupled versus decoupled reaching in the human brain. Strikingly, human brain activity associated with decoupled reach tended to occur within the rostral portion of PMd and the superior-caudal portion of SPL. Activity associated with coupled reaches was localized to the caudal portion of PMd and regions within SPL surrounding mIPS. This pattern of activity, parallel to our observations in nonhuman primates, not only supports our neurophysiological studies but also helps to bridge the gap between animal and human studies due to the strong relationship between LFPs and fMRI (Goense & Logothetis, 2008; Nir et al., 2007). Our findings emphasize the importance of accounting for the nature of eye–hand visuomotor mapping when interpreting movement control data.

Acknowledgments

We would like to thank Taiwo McGregor, Tyrone Lew, Dr. Xiaogang Yan, Dr. Bogdan Neagu, and Dr. Hongying Wang for their exceptional technical, surgical, and data collection assistance, as well as Natasha Down, Veronica Scavo, Julie Panakos, and Dr. Melissa Madden for their invaluable animal care expertise. We would also like to thank Dr. Hjalmar Turesson for his expert data analysis advice and guidance. This work was supported by Canadian Institutes of Health Research Grant MOP-74634 (L. S.), the Canadian Foundation for Innovation and the Ontario Innovation Trust (L. S.), and the Ontario Ministry of Training, Colleges, and Universities (OGSST to P. S.).

Reprint requests should be sent to Dr. Lauren E. Sergio, 4700 Keele Street, 357 Bethune College, Toronto, ON, Canada, M3J 1P3, or via e-mail: lsergio@yorku.ca.

REFERENCES

Abe, M., & Hanakawa, T. (2009). Functional coupling underlying motor and cognitive functions of the dorsal premotor cortex. *Behavioural Brain Research, 198,* 13–23.

Alexander, G. E., & Crutcher, M. D. (1990). Preparation for movement: Neural representations of intended direction in three motor areas of the monkey. *Journal of Neurophysiology, 64,* 133–150.

Andersen, R. A., Musallam, S., & Pesaran, B. (2004). Selecting the signals for a brain-machine interface. *Current Opinion in Neurobiology, 14,* 720–726.

Barbas, H., & Pandya, D. N. (1987). Architecture and frontal cortical connections of the premotor cortex (area 6) in the rhesus monkey. *Journal of Comparative Neurology, 256,* 211–228.

Bartos, M., Vida, I., & Jonas, P. (2007). Synaptic mechanisms of synchronized gamma oscillations in inhibitory interneuron networks. *Nature Reviews Neuroscience, 8,* 45–56.

Bastos, A. M., Usrey, W. M., Adams, R. A., Mangun, G. R., Fries, P., & Friston, K. J. (2012). Canonical microcircuits for predictive coding. *Neuron, 76,* 695–711.

Battaglia-Mayer, A., Ferrari-Toniolo, S., & Visco-Comandini, F. (2015). Timing and communication of parietal cortex for visuomotor control. *Current Opinion in Neurobiology, 33,* 103–109.

Battaglia-Mayer, A., Ferrari-Toniolo, S., Visco-Comandini, F., Archambault, P. S., Saberi-Moghadam, S., & Caminiti, R. (2013). Impairment of online control of hand and eye movements in a monkey model of optic ataxia. *Cerebral Cortex, 23,* 2644–2656.

Beurze, S. M., Toni, I., Pisella, L., & Medendorp, W. P. (2010). Reference frames for reach planning in human parietofrontal cortex. *Journal of Neurophysiology, 104,* 1736–1745.

Blangero, A., Ota, H., Delporte, L., Revol, P., Vindras, P., Rode, G., et al. (2007). Optic ataxia is not only "optic": Impaired spatial integration of proprioceptive information. *Neuroimage, 36(Suppl. 2),* T61–T68.

Bo, J., Contreras-Vidal, J. L., Kagerer, F. A., & Clark, J. E. (2006). Effects of increased complexity of visuo-motor transformations on children's arm movements. *Human Movement Science, 25,* 553–567.

Bosman, C. A., Schoffelen, J. M., Brunet, N., Oostenveld, R., Bastos, A. M., Womelsdorf, T., et al. (2012). Attentional stimulus selection through selective synchronization between monkey visual areas. *Neuron, 75,* 875–888.

Boussaoud, D. (2001). Attention versus intention in the primate premotor cortex. *Neuroimage, 14,* S40–S45.

Boussaoud, D., & Wise, S. P. (1993). Primate frontal cortex: Effects of stimulus and movement. *Experimental Brain Research, 95,* 28–40.

Breveglieri, R., Galletti, C., Gamberini, M., Passarelli, L., & Fattori, P. (2006). Somatosensory cells in area PEc of macaque posterior parietal cortex. *Journal of Neuroscience, 26,* 3679–3684.

Buneo, C. A., & Andersen, R. A. (2006). The posterior parietal cortex: Sensorimotor interface for the planning and online control of visually guided movements. *Neuropsychologia, 44,* 2594–2606.

Buschman, T. J., Denovellis, E. L., Diogo, C., Bullock, D., & Miller, E. K. (2012). Synchronous oscillatory neural ensembles for rules in the prefrontal cortex. *Neuron, 76,* 838–846.

Buschman, T. J., & Miller, E. K. (2007). Top–down versus bottom–up control of attention in the prefrontal and posterior parietal cortices. *Science, 315,* 1860–1862.

Buzsaki, G., Anastassiou, C. A., & Koch, C. (2012). The origin of extracellular fields and currents—EEG, ECoG, LFP and spikes. *Nature Reviews Neuroscience, 13,* 407–420.

Caminiti, R., Ferraina, S., & Mayer, A. B. (1998). Visuomotor transformations: Early cortical mechanisms of reaching. *Current Opinion in Neurobiology, 8,* 753–761.

Caminiti, R., Genovesio, A., Marconi, B., Mayer, A. B., Onorati, P., Ferraina, S., et al. (1999). Early coding of reaching: Frontal and parietal association connections of parieto-occipital cortex. *European Journal of Neuroscience, 11,* 3339–3345.

Caminiti, R., Johnson, P. B., Galli, C., Ferraina, S., & Burnod, Y. (1991). Making arm movements within different parts of space: The premotor and motor cortical representation of a coordinate system for reaching to visual targets. *Journal of Neuroscience, 11,* 1182–1197.

Cisek, P., Crammond, D. J., & Kalaska, J. F. (2003). Neural activity in primary motor and dorsal premotor cortex in reaching tasks with the contralateral versus ipsilateral arm. *Journal of Neurophysiology, 89,* 922–942.

Cisek, P., & Kalaska, J. F. (2002). Simultaneous encoding of multiple potential reach directions in dorsal premotor cortex. *Journal of Neurophysiology, 87,* 1149–1154.

Cisek, P., & Kalaska, J. F. (2005). Neural correlates of reaching decisions in dorsal premotor cortex: Specification of multiple direction choices and final selection of action. *Neuron, 45,* 801–814.

Clavagnier, S., Prado, J., Kennedy, H., & Perenin, M. T. (2007). How humans reach: Distinct cortical systems for central and peripheral vision. *The Neuroscientist, 13,* 22–27.

Colby, C. L. (1998). Action-oriented spatial reference frames in cortex. *Neuron, 20,* 15–24.

Colby, C. L., Duhamel, J. R., & Goldberg, M. E. (1996). Visual, presaccadic, and cognitive activation of single neurons in monkey lateral intraparietal area. *Journal of Neurophysiology, 76,* 2841–2852.

Connolly, J. D., Goodale, M. A., Desouza, J. F., Menon, R. S., & Vilis, T. (2000). A comparison of frontoparietal fMRI activation during anti-saccades and anti-pointing. *Journal of Neurophysiology, 84,* 1645–1655.

Culham, J. C., & Valyear, K. F. (2006). Human parietal cortex in action. *Current Opinion in Neurobiology, 16,* 205–212.

Desmurget, M., Gréa, H., Grethe, J. S., Prablanc, C., Alexander, G. E., & Grafton, S. T. (2001). Functional anatomy of nonvisual feedback loops during reaching: A positron emission tomography study. *Journal of Neuroscience, 21,* 2919–2928.

Eickhoff, S. B., Laird, A. R., Grefkes, C., Wang, L. E., Zilles, K., & Fox, P. T. (2009). Coordinate-based activation likelihood estimation meta-analysis of neuroimaging data: A random-effects approach based on empirical estimates of spatial uncertainty. *Human Brain Mapping, 30,* 2907–2926.

Engel, A. K., & Fries, P. (2010). Beta-band oscillations—Signalling the status quo? *Current Opinion in Neurobiology, 20,* 156–165.

Engel, K. C., Flanders, M., & Soechting, J. F. (2002). Oculocentric frames of reference for limb movement. *Archives Italiennes de Biologie, 140,* 211–219.

Fabbri, S., Caramazza, A., & Lingnau, A. (2010). Tuning curves for movement direction in the human visuomotor system. *Journal of Neuroscience, 30,* 13488–13498.

Fabbri, S., Strnad, L., Caramazza, A., & Lingnau, A. (2014). Overlapping representations for grip type and reach direction. *Neuroimage, 94,* 138–146.

Filimon, F., Nelson, J. D., Hagler, D. J., & Sereno, M. I. (2007). Human cortical representations for reaching: Mirror neurons for execution, observation, and imagery. *Neuroimage, 37,* 1315–1328.

Filimon, F., Nelson, J. D., Huang, R. S., & Sereno, M. I. (2009). Multiple parietal reach regions in humans: Cortical representations for visual and proprioceptive feedback during on-line reaching. *Journal of Neuroscience, 29,* 2961–2971.

Filimon, F., Rieth, C. A., Sereno, M. I., & Cottrell, G. W. (2014). Observed, executed, and imagined action representations can be decoded from ventral and dorsal areas. *Cerebral Cortex*.

Flanders, M., Helms-Tillery, S. I., & Soechting, J. F. (1992). Early stages in the sensorimotor transformation. *Behavioral and Brain Sciences, 15,* 309–362.

Fries, P. (2005). A mechanism for cognitive dynamics: Neuronal communication through neuronal coherence. *Trends in Cognitive Sciences, 9,* 474–480.

Fujii, N., Mushiake, H., & Tanji, J. (2000). Rostrocaudal distinction of the dorsal premotor area based on oculomotor involvement. *Journal of Neurophysiology, 83,* 1764–1769.

Gail, A., Klaes, C., & Westendorff, S. (2009). Implementation of spatial transformation rules for goal-directed reaching via gain modulation in monkey parietal and premotor cortex. *Journal of Neuroscience, 29,* 9490–9499.

Gallivan, J. P., McLean, D. A., Smith, F. W., & Culham, J. C. (2011). Decoding effector-dependent and effector-independent movement intentions from human parieto-frontal brain activity. *Journal of Neuroscience, 31,* 17149–17168.

Gauthier, G. M., & Mussa Ivaldi, F. (1988). Oculo-manual tracking of visual targets in monkey: Role of the arm afferent information in the control of arm and eye movements. *Experimental Brain Research, 73,* 138–154.

Ghilardi, M. F., Alberoni, M., Marelli, S., Rossi, M., Franceschi, M., Ghez, C., et al. (1999). Impaired movement control in Alzheimer's disease. *Neuroscience Letters, 260,* 45–48.

Goense, J. B., & Logothetis, N. K. (2008). Neurophysiology of the BOLD fMRI signal in awake monkeys. *Current Biology, 18,* 631–640.

Gorbet, D. J., & Sergio, L. E. (2007). Preliminary sex differences in human cortical BOLD fMRI activity during the preparation of increasingly complex visually guided movements. *European Journal of Neuroscience, 25,* 1228–1239.

Gorbet, D. J., & Sergio, L. E. (2009). The behavioural consequences of dissociating the spatial directions of eye and arm movements. *Brain Research, 1284,* 77–88.

Gorbet, D. J., & Sergio, L. E. (2016). Don't watch where you're going: The neural correlates of decoupling eye and arm movements. *Behavioural Brain Research, 298,* 229–240.

Gorbet, D. J., Staines, W. R., & Sergio, L. E. (2004). Brain mechanisms for preparing increasingly complex sensory to motor transformations. *Neuroimage, 23,* 1100–1111.

Grafton, S. T., Fagg, A. H., Woods, R. P., & Arbib, M. A. (1996). Functional anatomy of pointing and grasping in humans. *Cerebral Cortex, 6,* 226–237.

Grafton, S. T., Hazeltine, E., & Ivry, R. B. (1998). Abstract and effector-specific representations of motor sequences identified with PET. *Journal of Neuroscience, 18,* 9420–9428.

Granek, J. A., Gorbet, D. J., & Sergio, L. E. (2010). Extensive video-game experience alters cortical networks for complex visuomotor transformations. *Cortex, 46,* 1165–1177.

Granek, J. A., Pisella, L., Blangero, A., Rossetti, Y., & Sergio, L. E. (2012). The role of the caudal superior parietal lobule in updating hand location in peripheral vision: Further evidence from optic ataxia. *PLoS One, 7,* e46619.

Granek, J. A., & Sergio, L. E. (2013). Disrupting the integration of a cognitive rule into a motor action in decoupled eye–hand coordination using a dual task paradigm. *PLoS One,* in revision.

Granek, J. A., & Sergio, L. E. (2015). Evidence for distinct brain networks in the control of rule-based motor behavior. *Journal of Neurophysiology, 114,* 1298–1309.

Grea, H., Pisella, L., Rossetti, Y., Desmurget, M., Tilikete, C., Grafton, S., et al. (2002). A lesion of the posterior parietal cortex disrupts on-line adjustments during aiming movements. *Neuropsychologia, 40,* 2471–2480.

Haaland, K. Y., Elsinger, C. L., Mayer, A. R., Durgerian, S., & Rao, S. M. (2004). Motor sequence complexity and performing hand produce differential patterns of hemispheric lateralization. *Journal of Cognitive Neuroscience, 16,* 621–636.

Halsband, U., & Passingham, R. (1982). The role of premotor and parietal cortex in the direction of action. *Brain Research, 240,* 368–372.

Halsband, U., & Passingham, R. E. (1985). Premotor cortex and the conditions for movement in monkeys (*Macaca fascicularis*). *Behavioural Brain Research, 18,* 269–277.

Hawkins, K. M., Sayegh, P., Yan, X., Crawford, J. D., & Sergio, L. E. (2013). Neural activity in superior parietal cortex during rule-based visual-motor transformations. *Journal of Cognitive Neuroscience, 25,* 436–454.

Hawkins, K. M., & Sergio, L. E. (2014). Visuomotor impairments in older adults at increased Alzheimer's disease risk. *Journal of Alzheimer's Disease, 42,* 607–621.

Henriques, D. Y., Klier, E. M., Smith, M. A., Lowy, D., & Crawford, J. D. (1998). Gaze-centered remapping of remembered visual space in an open-loop pointing task. *Journal of Neuroscience, 18,* 1583–1594.

Hinkley, L. B., Nagarajan, S. S., Dalal, S. S., Guggisberg, A. G., & Disbrow, E. A. (2011). Cortical temporal dynamics of visually guided behavior. *Cerebral Cortex, 21,* 519–529.

Jackson, S. R., Newport, R., Husain, M., Fowlie, J. E., O'Donoghue, M., & Bajaj, N. (2009). There may be more to reaching than meets the eye: Re-thinking optic ataxia. *Neuropsychologia, 47,* 1397–1408.

Jarvis, M. R., & Mitra, P. P. (2001). Sampling properties of the spectrum and coherency of sequences of action potentials. *Neural Computation, 13,* 717–749.

Johnson, P. B., Ferraina, S., Bianchi, L., & Caminiti, R. (1996). Cortical networks for visual reaching: Physiological and anatomical organization of frontal and parietal lobe arm regions. *Cerebral Cortex, 6,* 102–119.

Kalaska, J. F., Caminiti, R., & Georgopoulos, A. P. (1983). Cortical mechanisms related to the direction of two-dimensional arm movements: Relations in parietal area 5 and comparison with motor cortex. *Experimental Brain Research, 51,* 247–260.

Kalaska, J. F., Cohen, D. A., Hyde, M. L., & Prud'homme, M. (1989). A comparison of movement direction-related versus load direction-related activity in primate motor cortex, using a two-dimensional reaching task. *Journal of Neuroscience, 9,* 2080–2102.

Kalaska, J. F., Sergio, L. E., & Cisek, P. (1998). Cortical control of whole-arm motor tasks. *Novartis Foundation Symposia, 218,* 176–201.

Kertzman, C., Schwarz, U., Zeffiro, T. A., & Hallett, M. (1997). The role of posterior parietal cortex in visually guided reaching movements in humans. *Experimental Brain Research, 114,* 170–183.

Kurata, K. (1989). Motor programming in the premotor cortex of monkeys (pp. 39–47).

Kurata, K., & Hoffman, D. S. (1994). Differential effects of muscimol microinjection into dorsal and ventral aspects of the premotor cortex of monkeys. *Journal of Neurophysiology, 71,* 1151–1164.

Laird, A. R., Fox, P. M., Price, C. J., Glahn, D. C., Uecker, A. M., Lancaster, J. L., et al. (2005). ALE meta-analysis: Controlling the false discovery rate and performing statistical contrasts. *Human Brain Mapping, 25,* 155–164.

Lancaster, J. L., Woldorff, M. G., Parsons, L. M., Liotti, M., Freitas, C. S., Rainey, L., et al. (2000). Automated Talairach atlas labels for functional brain mapping. *Human Brain Mapping, 10,* 120–131.

Lee, J. H., & van Donkelaar, P. (2006). The human dorsal premotor cortex generates on-line error corrections during sensorimotor adaptation. *Journal of Neuroscience, 26,* 3330–3334.

Lu, M. T., Preston, J. B., & Strick, P. L. (1994). Interconnections between the prefrontal cortex and the premotor areas in the frontal lobe. *Journal of Comparative Neurology, 341,* 375–392.

Luppino, G., Rozzi, S., Calzavara, R., & Matelli, M. (2003). Prefrontal and agranular cingulate projections to the dorsal premotor areas F2 and F7 in the macaque monkey. *European Journal of Neuroscience, 17,* 559–578.

Maier, A., Adams, G. K., Aura, C., & Leopold, D. A. (2010). Distinct superficial and deep laminar domains of activity in the visual cortex during rest and stimulation. *Frontiers in Systems Neuroscience, 4*.

Marconi, B., Genovesio, A., Battaglia-Mayer, A., Ferraina, S., Squatrito, S., Molinari, M., et al. (2001). Eye–hand coordination during reaching. I. Anatomical relationships between parietal and frontal cortex. *Cerebral Cortex, 11,* 513–527.

Matelli, M., Camarda, R., Glickstein, M., & Rizzolatti, G. (1986). Afferent and efferent projections of the inferior area 6 in the macaque monkey. *Journal of Comparative Neurology, 251,* 281–298.

Mayka, M. A., Corcos, D. M., Leurgans, S. E., & Vaillancourt, D. E. (2006). Three-dimensional locations and boundaries of motor and premotor cortices as defined by functional brain imaging: A meta-analysis. *Neuroimage, 31,* 1453–1474.

Mountcastle, V. B., Lynch, J. C., Georgopoulos, A., Sakata, H., & Acuna, C. (1975). Posterior parietal association cortex of the monkey: Command functions for operations within extrapersonal space. *Journal of Neurophysiology, 38,* 871–908.

Murray, E. A., Bussey, T. J., & Wise, S. P. (2000). Role of prefrontal cortex in a network for arbitrary visuomotor mapping. *Experimental Brain Research, 133,* 114–129.

Nir, Y., Fisch, L., Mukamel, R., Gelbard-Sagiv, H., Arieli, A., Fried, I., et al. (2007). Coupling between neuronal firing rate, gamma LFP, and BOLD fMRI is related to interneuronal correlations. *Current Biology, 17,* 1275–1285.

Paxinos, G., Huang, X. F., & Toga, A. W. (2000). *The rhesus monkey brain in stereotaxic coordinates*. San Diego, CA: Academic Press.
Perenin, M. T., & Vighetto, A. (1988). Optic ataxia: A specific disruption in visuomotor mechanisms. I. Different aspects of the deficit in reaching for objects. *Brain, 111,* 643–674.
Pesaran, B., Nelson, M. J., & Andersen, R. A. (2006). Dorsal premotor neurons encode the relative position of the hand, eye, and goal during reach planning. *Neuron, 51,* 125–134.
Pesaran, B., Nelson, M. J., & Andersen, R. A. (2008). Free choice activates a decision circuit between frontal and parietal cortex. *Nature, 453,* 406–409.
Pesaran, B., Pezaris, J. S., Sahani, M., Mitra, P. P., & Andersen, R. A. (2002). Temporal structure in neuronal activity during working memory in macaque parietal cortex. *Nature Neuroscience, 5,* 805–811.
Petrides, M., & Pandya, D. N. (1999). Dorsolateral prefrontal cortex: Comparative cytoarchitectonic analysis in the human and macaque brain and corticocortical connection patterns. *European Journal of Neuroscience, 11,* 1011–1036.
Piaget, J. (1965). *The construction of reality in the child*. New York: Basic Books, Inc.
Picard, N., & Strick, P. L. (2001). Imaging the premotor areas. *Current Opinion in Neurobiology, 11,* 663–672.
Pisella, L., Sergio, L., Blangero, A., Torchin, H., Vighetto, A., & Rossetti, Y. (2009). Optic ataxia and the function of the dorsal stream: Contributions to perception and action. *Neuropsychologia, 47,* 3033–3044.
Prado, J., Clavagnier, S., Otzenberger, H., Scheiber, C., Kennedy, H., & Perenin, M. T. (2005). Two cortical systems for reaching in central and peripheral vision. *Neuron, 48,* 849–858.
Raos, V., Umilta, M. A., Gallese, V., & Fogassi, L. (2004). Functional properties of grasping-related neurons in the dorsal premotor area F2 of the macaque monkey. *Journal of Neurophysiology, 92,* 1990–2002.
Ray, S. (2015). Challenges in the quantification and interpretation of spike-LFP relationships. *Current Opinion in Neurobiology, 31,* 111–118.
Rizzolatti, G., Luppino, G., & Matelli, M. (1998). The organization of the cortical motor system: New concepts. *Electroencephalography and Clinical Neurophysiology, 106,* 283–296.
Roberts, M. J., Lowet, E., Brunet, N. M., Ter Wal, M., Tiesinga, P., Fries, P., et al. (2013). Robust gamma coherence between macaque V1 and V2 by dynamic frequency matching. *Neuron, 78,* 523–536.
Rossetti, Y., Revol, P., McIntosh, R., Pisella, L., Rode, G., Danckert, J., et al. (2005). Visually guided reaching: Bilateral posterior parietal lesions cause a switch from fast visuomotor to slow cognitive control. *Neuropsychologia, 43,* 162–177.
Rushworth, M. F., Nixon, P. D., & Passingham, R. E. (1997). Parietal cortex and movement. II. Spatial representation. *Experimental Brain Research, 117,* 311–323.
Saalmann, Y. B., Pigarev, I. N., & Vidyasagar, T. R. (2007). Neural mechanisms of visual attention: How top–down feedback highlights relevant locations. *Science, 316,* 1612–1615.
Salek, Y., Anderson, N. D., & Sergio, L. (2011). Mild cognitive impairment is associated with impaired visual-motor planning when visual stimuli and actions are incongruent. *European Neurology, 66,* 283–293.
Sayegh, P. F., Hawkins, K. M., Hoffman, K. L., & Sergio, L. E. (2013). Differences in spectral profiles between rostral and caudal premotor cortex when hand-eye actions are decoupled. *Journal of Neurophysiology, 110,* 952–963.
Sayegh, P. F., Hawkins, K. M., Neagu, B., Crawford, J. D., Hoffman, K. L., & Sergio, L. E. (2014). Decoupling the actions of the eyes from the hand alters beta and gamma synchrony within SPL. *Journal of Neurophysiology, 111,* 2210–2221.
Sergio, L. E., Gorbet, D. J., Tippett, W. J., Yan, X., & Neagu, B. (2009). Cortical mechanisms of vision for complex action. In M. Jenkins & L. Harris (Eds.), *Cortical mechanisms of vision*. Cambridge: Cambridge University Press.
Sergio, L. E., & Scott, S. H. (1998). Hand and joint paths during reaching movements with and without vision. *Experimental Brain Research, 122,* 157–164.
Singhal, A., Monaco, S., Kaufman, L. D., & Culham, J. C. (2013). Human fMRI reveals that delayed action re-recruits visual perception. *PLoS One, 8,* e73629.
Spaak, E., Bonnefond, M., Maier, A., Leopold, D. A., & Jensen, O. (2012). Layer-specific entrainment of gamma-band neural activity by the alpha rhythm in monkey visual cortex. *Current Biology, 22,* 2313–2318.
Stetson, C., & Andersen, R. A. (2014). The parietal reach region selectively anti-synchronizes with dorsal premotor cortex during planning. *Journal of Neuroscience, 34,* 11948–11958.
Tachibana, Y., Nambu, A., Hatanaka, N., Miyachi, S., & Takada, M. (2004). Input–output organization of the rostral part of the dorsal premotor cortex, with special reference to its corticostriatal projection. *Neuroscience Research, 48,* 45–57.
Tanne-Gariepy, J., Rouiller, E. M., & Boussaoud, D. (2002). Parietal inputs to dorsal versus ventral premotor areas in the macaque monkey: Evidence for largely segregated visuomotor pathways. *Experimental Brain Research, 145,* 91–103.
Terao, Y., Andersson, N. E., Flanagan, J. R., & Johansson, R. S. (2002). Engagement of gaze in capturing targets for future sequential manual actions. *Journal of Neurophysiology, 88,* 1716–1725.
Thoenissen, D., Zilles, K., & Toni, I. (2002). Differential involvement of parietal and precentral regions in movement preparation and motor intention. *Journal of Neuroscience, 22,* 9024–9034.
Tippett, W. J., & Sergio, L. E. (2006). Visuomotor integration is impaired in early stage Alzheimer's disease. *Brain Research, 1102,* 92–102.
Toni, I., Shah, N. J., Fink, G. R., Thoenissen, D., Passingham, R. E., & Zilles, K. (2002). Multiple movement representations in the human brain: An event-related fMRI study. *Journal of Cognitive Neuroscience, 14,* 769–784.
Tunik, E., Saleh, S., & Adamovich, S. V. (2013). Visuomotor discordance during visually-guided hand movement in virtual reality modulates sensorimotor cortical activity in healthy and hemiparetic subjects. *IEEE Transactions on Neural Systems and Rehabilitation Engineering, 21,* 198–207.
Turesson, H. K., Logothetis, N. K., & Hoffman, K. L. (2012). Category-selective phase coding in the superior temporal sulcus. *Proceedings of the National Academy of Sciences, U.S.A., 109,* 19438–19443.
Turkeltaub, P. E., Eden, G. F., Jones, K. M., & Zeffiro, T. A. (2002). Meta-analysis of the functional neuroanatomy of single-word reading: Method and validation. *Neuroimage, 16,* 765–780.
Turkeltaub, P. E., Eickhoff, S. B., Laird, A. R., Fox, M., Wiener, M., & Fox, P. (2012). Minimizing within-experiment and within-group effects in activation likelihood estimation meta-analyses. *Human Brain Mapping, 33,* 1–13.
Vercher, J. L., Magenes, G., Prablanc, C., & Gauthier, G. M. (1994). Eye-head-hand coordination in pointing at visual targets: Spatial and temporal analysis. *Experimental Brain Research, 99,* 507–523.
Vesia, M., & Crawford, J. D. (2012). Specialization of reach function in human posterior parietal cortex. *Experimental Brain Research, 221,* 1–18.

Vinck, M., Womelsdorf, T., Buffalo, E. A., Desimone, R., & Fries, P. (2013). Attentional modulation of cell-class-specific gamma-band synchronization in awake monkey area v4. *Neuron, 80,* 1077–1089.

Wise, S. P., di Pellegrino, G., & Boussaoud, D. (1996). The premotor cortex and nonstandard sensorimotor mapping. *Canadian Journal of Physiology and Pharmacology, 74,* 469–482.

Womelsdorf, T., & Fries, P. (2006). Neuronal coherence during selective attentional processing and sensory-motor integration. *Journal of Physiology, Paris, 100,* 182–193.

Womelsdorf, T., Fries, P., Mitra, P. P., & Desimone, R. (2006). Gamma-band synchronization in visual cortex predicts speed of change detection. *Nature, 439,* 733–736.

Womelsdorf, T., Schoffelen, J. M., Oostenveld, R., Singer, W., Desimone, R., Engel, A. K., et al. (2007). Modulation of neuronal interactions through neuronal synchronization. *Science, 316,* 1609–1612.

Wu, W., Wheeler, D. W., Staedtler, E. S., Munk, M. H., & Pipa, G. (2008). Behavioral performance modulates spike field coherence in monkey prefrontal cortex. *NeuroReport, 19,* 235–238.